Colloid Polym Sci 278:736–745 (2000)

ORIGINAL CONTRIBUTION

C. J. G. Plummer
J. Kiefer

Predicting the phase behaviour of solvent-modified epoxy resins

Received: 20 September 1999
Accepted: 21 December 1999

C. J. G. Plummer (✉)
Laboratoire de Polymères
Ecole Polytechnique Fédérale de Lausanne
1015 Lausanne, Switzerland
e-mail: christopher.plummer@epfl.ch
Tel.: +41-21-6932856
Fax: +41-21-6935868

J. Kiefer
Paul-Scherrer-Institut
5232 Villigen-PSI, Switzerland

Abstract The Flory–Huggins equation has been used to model the equilibrium phase behaviour of a solvent-modified epoxy resin intended for the fabrication of porous components by chemically induced phase separation followed by evacuation of the solvent after curing. Points in composition–temperature space corresponding to a transition from homogeneous to heterogeneous postcuring microstructures have been identified for a variety of solvents using a thermal gradient oven. Assuming this transition to coincide with the cloud-point curve corresponding to the gel point of the resin, the data were used in conjunction with the predictions of the Flory–Huggins equation to estimate the interaction parameter and its temperature dependence for each solvent. Phase diagrams in composition–conversion space were then calculated for a range of curing temperatures.

Key words Epoxy resin · Chemically induced phase separation interaction parameter · Flory–Huggins

Introduction

Chemically induced phase separation (CIPS) is a potentially versatile means of producing porous thermosets as has been demonstrated for epoxy- and cyanurate-based materials [1–4]. CIPS often occurs during the curing of an initially soluble mixture of an epoxy resin and a low-molecular-weight solvent, mainly as a consequence of the increase in molecular weight of the resin and the accompanying decrease in the entropy of mixing. The solvent may then be removed by evaporation to give a porous solid. The aim of the present work is to obtain a working approximation to the equilibrium phase behaviour in such systems using a simple method for estimating the interaction parameter, χ, based on the assumption that phase separation becomes inhibited when the degree of cross-linking exceeds the gel point and that χ depends only on temperature. Although this latter assumption may be questionable [5], particularly in systems showing strong specific interactions [6, 7], the present approach is anticipated to be of wide interest for microstructural control in porous thermosets, since the attainable degrees of porosity as well as the pore size and connectivity depend strongly on the evolution of the miscibility with solvent content and the extent of curing [2, 4]. However, the discussion will be limited here to the specific case of diglycidyl ether of bisphenol A (DGEBA) (M_r = 340 g/mol) cured with *p*-aminocyclohexylpropane (PACP) (M_r = 234 g/mol) and modified with a number of different solvents. Moreover, to maintain simplicity, a statistical model is used to calculate the moments of the molecular-weight distribution as a function of the extent of curing. This provides a reasonable first approximation to the behaviour of systems such as DGEBA/PACP that have relatively simple reaction paths, providing an indication of the divergence of the number- and weight-average molar masses at the gel point. However, in a more detailed approach, and in the case of more complex

systems, it would be necessary to take into account local changes in reactivity and mobility within a more flexible framework, such as that provided by a kinetic model [8, 9].

Thermodynamics

According to the Flory–Huggins theory, the free energy of mixing, ΔG_m, of a binary blend is given by [10, 11]

$$\frac{\Delta G_m}{kT} = \frac{\phi_A}{N_A}\ln\phi_A + \frac{\phi_B}{N_B}\ln\phi_B + \chi\phi_A\phi_B \quad , \tag{1}$$

where ϕ_A and ϕ_B and N_A and N_B are the volume fraction and effective degree of polymerization of the respective components (N is the number of lattice sites in the Flory–Huggins model occupied by a given molecule). The qualitative, and in some cases, quantitative behaviour of binary blends may usually be accounted for by Eq. (1), in so far as the components may be considered to be monodisperse. If only one of the components is monodisperse, Eq. (1) may be replaced by [12]

$$\frac{\Delta G_m}{kT} = \sum_i \frac{\phi_{Ai}}{N_{Ai}}\ln\phi_{Ai} + \frac{\phi_B}{N_B}\ln\phi_B + \chi(1-\phi_B)\phi_B \quad , \tag{2}$$

where ϕ_{Ai} is the volume fraction of molecules of A with an effective degree of polymerization N_{Ai} and ϕ_B is the volume of the monodisperse component, which we shall henceforth refer to as the solvent.

Equation 2 is particularly appropriate to blends containing thermosets, in which high degrees of polydispersity are anticipated at degrees of conversion approaching the gel point [9]. However, an idea of the size distribution of the resin at any given point in the reaction is needed. To obtain this, we adopt a statistical model based on the assumption that all functional groups react with equal probability, α.

In the present case, if $P(N,M)$ is the probability that a given molecule in a partly cured stoichiometric mixture of DGEBA and PACP contains N PACP and M DGEBA molecules, the corresponding volume fraction of such molecules is

$$\phi_{N,M} = \frac{NV_{PACP} + MV_{DGEBA}}{N(2V_{DGEBA} + V_{PACP})}P(N,M); \qquad N \geq 1,\ N-1 \leq M \leq 3N+1,$$

$$\phi_{0,1} = 2V_{DGEBA}/(2V_{DGEBA} + V_{PACP})P(0,1) \quad , \tag{3}$$

where V are the molar volumes of each component. By considering all the possible ways of forming a molecule containing N PACP and M DGEBA molecules (intramolecular reactions are ignored), it may be shown that

$$P(N,M) = \frac{4(3N)!(1-\alpha)^{2N+2}\alpha^{2N-2}}{(N-1)!(2N+2)!} \times \left(\frac{(2N+2)!}{(3N+1-M)!(M-N+1)!}\alpha^{M-N+1}\right); \qquad N \geq 1,\ N-1 \leq M \leq 3N+1$$

$$P(0,1) = (1-\alpha)^2 \quad . \tag{4}$$

and that

$$P(N) = \sum_{M=N-1}^{3N+1} P(N,M) = \frac{4(3N)!\alpha^{2(N-1)}(1-\alpha^2)^{2N+2}}{(N-1)!(2N+2)!} \quad , \tag{5}$$

which is equivalent to the expression given by Flory and Stockmayer [13, 14] for the volume fraction of molecules with a degree of polymerization, N, resulting from the condensation of identical tetrafunctional monomers (here α^2 is effectively equal to the probability that two functional groups belonging to two of these molecules react).

Equation 2 may now be written

$$\frac{\Delta G_m}{kT} = \sum_N \sum_{M=N-1}^{3N+1} \frac{(1-\phi_B)\phi_{N,M}}{N_{N,M}}\ln[(1-\phi_B)\phi_{N,M}] + \frac{\phi_B}{N_B}\ln\phi_B + \chi(1-\phi_B)\phi_B \quad , \tag{6}$$

where $N_{N,M} = (NV_{PACP} + MV_{DGEBA})/V_o$ and V_o is the volume corresponding to a lattice site in the Flory–Huggins model. Combining Eqs. (3)–(5) gives

$$\phi_{N,M} = \frac{NV_{PACP} + MV_{DGEBA}}{N(2V_{DGEBA} + V_{PACP})}P(N)f(M) \quad , \tag{7}$$

with $f(M) = P(N,M)/P(N)$ being defined by Eqs. (4) and (5). Setting $V_B/V_o = n_s$ and $(2V_{DGEBA} + V_{PACP})/V_B = n_e$ the first term on the right-hand side of Eq. (6) becomes

$$\sum_N \frac{1-\phi_B}{n_s n_e N} \sum_{M=N-1}^{3N+1} P(N)f(M) \times \left[\ln\left(\frac{N_{N,M}}{n_s n_e N}\right) + \ln P(N) + \ln f(M) + \ln(1-\phi_B)\right]$$

$$= \sum_N \frac{1-\phi_B}{n_s n_e N}P(N)\left\{\ln[(1-\phi_B)P(N)] + \sum_{M=N-1}^{3N+1} f(M)\left[\ln\left(\frac{N_{N,M}}{n_s n_e N}\right) + \ln f(M)\right]\right\} \quad .$$

As α tends to $\alpha_c = (1/3)^{1/2} \approx 0.58$, which defines the gel point, the terms in M become negligible and in place of Eq. (6) we obtain

$$\frac{n_s \Delta G_m}{kT} \approx \frac{(1-\phi_B)}{n_e} \sum_N \frac{P(N)}{N} \ln[(1-\phi_B)P(N)] + \phi_B \ln \phi_B + n_s \chi (1-\phi_B)\phi_B \quad . \tag{8}$$

Assuming χ to be independent of composition, either Eq. (6) or Eq. (8) may be used to estimate the cloud-point curves close to the gel point, following the approach of Clarke et al. [15] briefly outlined in the Appendix. As well as being relatively simple, Eq. (8) has the advantage that a simple power-law approximation may be substituted for $P(N)$, so the cloud-point curve at the gel point, which is of particular importance for the following section, may be derived in a straightforward manner. On the other hand, Eq. (6) is more appropriate for estimating cloud-point curves at lower degrees of conversion, where the terms in M can no longer be neglected. Critical points, ϕ_c, and spinodal curves are calculated from either $\phi_{N,M}$ or $P(N)$, again as described in the Appendix. The spinodal curve provides a convenient check of the calculated cloud-point curve at α_c since it should be asymptotic to this latter as α tends to α_c for modifier contents greater than ϕ_c [15].

Experimental

A stoichiometric blend of DGEBA (DER332 from Dow) and PACP (HY2954 from Ciba-Geigy) was mixed with analysis grades of hexane, octane, decane, cyclohexane, methylcyclohexane or 2,6-dimethyl-4-heptanone in the required proportions. The mixtures were then transferred to a 5-mm-diameter glass tube sealed at one end and stored in liquid N_2. After sealing the other end of the glass tube under vacuum, each sample was homogenized by brief heating in a silicon oil bath at 60 °C. The tube was then placed in a thermal gradient oven, a schematic representation of which is given in Fig. 1.

The temperature gradient was maintained by cooling one end of the oven with water and by placing the other end in contact with a hot plate with an integrated thermocouple, allowing temperature control to within 1 K. The temperature of the tube was estimated using thermocouples inserted at regular intervals along the oven wall and connected to a multichannel data logger (Kontron Poly-Rec30 + 5). By thermally insulating the oven walls a linear temperature gradient was obtained over the entire length of the sample [4].

After heat treatment, uncoated samples were examined after fracture in liquid N_2 using a Philips XL30 scanning electron microscope equipped with a field emission gun operating at about 1 kV.

Results

Estimating the interaction parameter

χ in polymer–solvent systems is generally temperature dependent. This may result in either an upper critical solution temperature or a lower critical solution temperature, depending on whether χ decreases or increases with temperature. However, for the model epoxy–solvent system under consideration here, the miscibility of the resin was observed to increase with temperature for all the solvents investigated, so phase separation was expected to occur at progressively higher α as the curing temperature was raised, as shown schematically in Fig. 2.

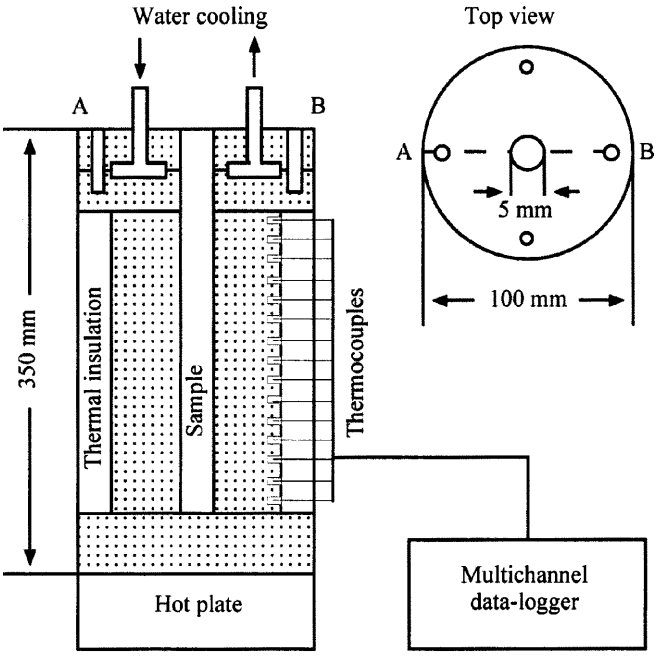

Fig. 1 Schematic representation of the thermal gradient oven

Using the thermal gradient oven, it was found that within certain ranges of solvent content there was a critical temperature, $T_c(\phi_B)$, above which no phase separation occurred even after curing was complete. It was assumed that this corresponded to the intercept of the cloud-point curve with the gel-point line as shown in Fig. 2 (the rapid increase in viscosity as α approaches α_c is expected to suppress nucleation of second phase domains). Hence by calculating the cloud-point curve in $\phi_B, n_s\chi$ space corresponding to $\alpha = \alpha_c$ in a given system and combining this with the T_c data shown in Fig. 3, $n_s\chi$ could be estimated as a function of temperature (assuming it to be independent of composition). In other words, if $n_s\chi_c(\phi_B)$ are points on the calculated cloud-point curve for $\alpha = \alpha_c$, then given $T_c(\phi_B)$, one can obtain $n_s\chi_c(T_c)$, which is necessarily a subset of $n_s\chi(T)$.

For all the solvents it was found that

$$n_s\chi = A + B/T \tag{9}$$

provided a convenient analytical description of the derived interaction parameter, where A and B are adjustable parameters. In Fig. 4, best-fit values of A and B have been used to recalculate $n_s\chi_c(\phi_B)$ from $A + B/T_c(\phi_B)$ and the results are compared with the calculated cloud-point curve for the epoxy–decane system and $\alpha = \alpha_c$. Since all the solvents investigated had similar molar volumes, their calculated cloud-point curves were very close in the range of compositions

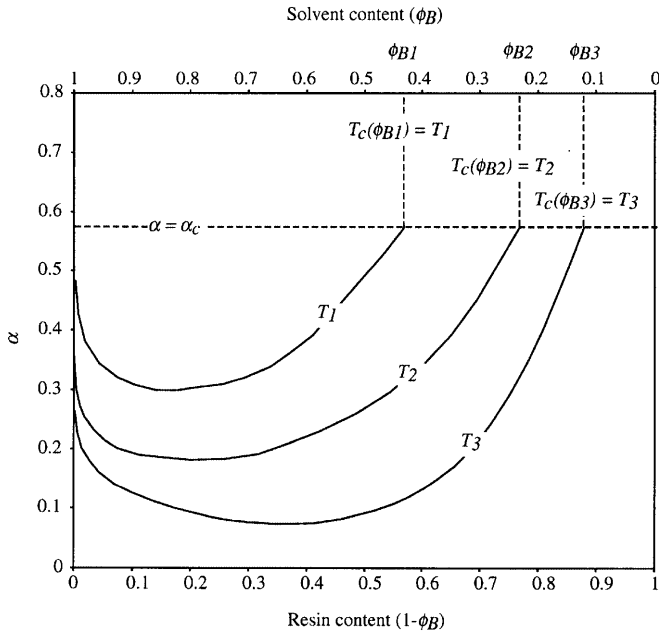

Fig. 2 Schematic of the form of the cloud-point curves in ϕ_B, α space for $T_1 > T_2 > T_3$. Phase separation is assumed to be inhibited at all T_c, where T_c is the temperature at which the cloud-point curve crosses the gel-point conversion line for a given composition. This composition may be identified with a value of $n_s\chi$ by calculating the cloud-point curve in $\phi_B, n_s\chi$ space for $\alpha = \alpha_c$. T_c is determined using the temperature gradient oven

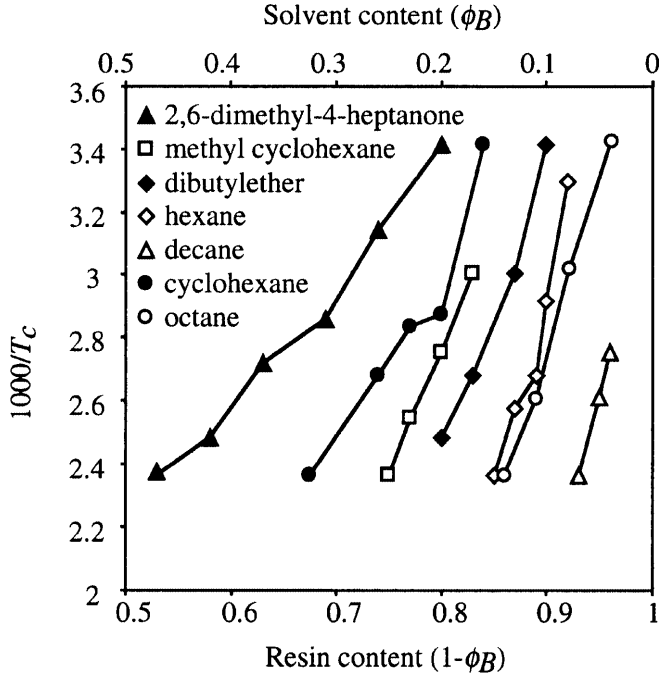

Fig. 3 $1/T_c$ versus $1 - \phi_B$ for different solvents measured using the thermal gradient oven. For $1 - \phi_B$ to the *left* of a given curve, no phase separation is observed after curing for that solvent

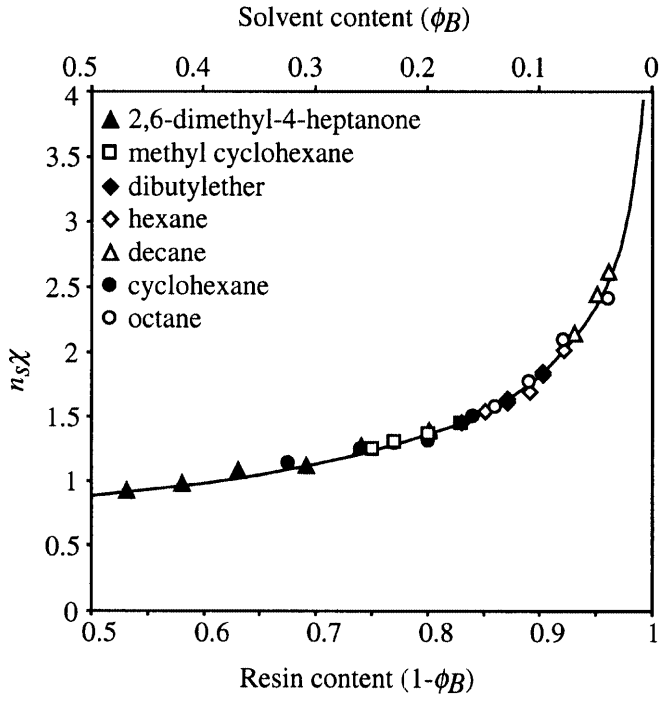

Fig. 4 The calculated cloud-point curve corresponding to the gel point in a decane-modified epoxy resin, onto which the data in Fig. 3 have been superposed as described in the text

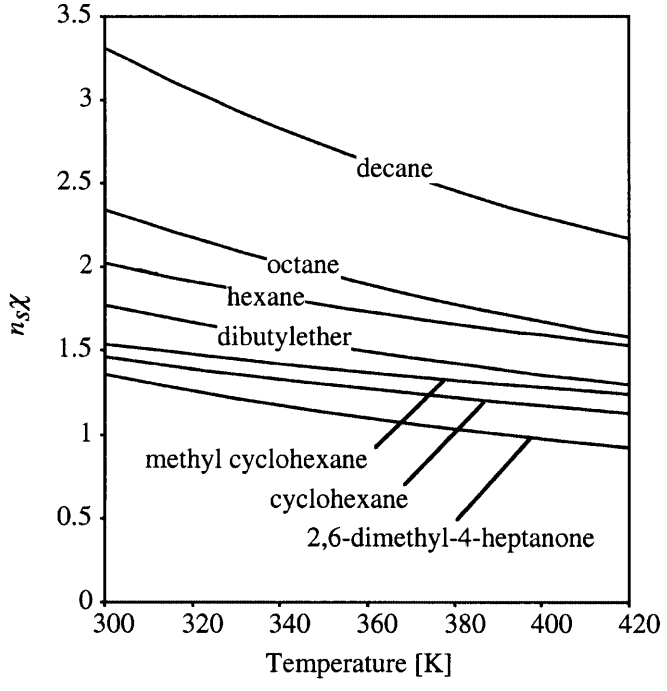

Fig. 5 Estimated values of $n_s\chi$ from Eq. (9) for different solvents plotted against temperature

shown, accounting for the apparent superposition of the data points in this figure. Finally, $n_s\chi(T)$ are compared in Fig. 5 for all the solvents considered.

Table 1 gives values of χ calculated from solubility parameters, estimated in turn from group contribution theory as described elsewhere [2, 4], an approach which is currently widely used for polymer-based systems [16]. Also given in Table 1 are room temperature values of $n_s\chi/V_B$ estimated from the data. To make the comparison meaningful both sets of values have been normalized by dividing by the respective values obtained for hexane. Reasonable agreement is obtained for the linear alkane series, for which both the solubility parameter approach and the present model are expected to provide relatively good descriptions (owing to the absence of specific solvent–resin interactions and the comparable architecture). The agreement is also reasonable for the more polar solvent dibutyl ether, but it is less good for 2,6-dimethyl-4-heptanone, cyclohexane and methylcyclohexane. A simple explanation for this in terms of the solubility parameter approach is that the comparison in Table 1 implicitly assumes V_o to be identical for all the solvents, whereas the conformational freedom of 2,6-dimethyl-4-heptanone, cyclohexane and methylcyclohexane will be restricted with respect to that of the linear molecules, and this assumption becomes questionable. One would anticipate a higher effective V_o for cyclohexane than for hexane, for example, leading to a lower value of χ/χ_{hexane} than given in Table 1.

Such problems do not arise when $n_s\chi$ is estimated from T_c since V_o is not required to calculate the cloud-point curves. Thus there is a progressive decrease in $V_{hexane}n_s\chi/V_Bn_{s,hexane}\chi_{hexane}$ on going from hexane to cyclohexane to methylcyclohexane, which is assumed to reflect the progressively more limited conformational freedom. Similarly, although the solubility parameter approach suggests dibutyl ether to be a better solvent than 2,6-dimethyl-4-heptanone, this would be offset by the more limited conformational freedom of the latter. Nevertheless, it should be borne in mind that particularly in the case of the more polar solvents, the assumption that χ is independent of composition is difficult to maintain.

Phase diagram predictions

In the remainder of this section we shall discuss the predicted phase diagrams in the light of the estimated temperature dependence of $n_s\chi$ for the different solvents. Representative cloud-point curves in $\phi_B, n_s\chi$ space are shown in Fig. 6 for different values of $\alpha \leq \alpha_c$ and for the decane epoxy mixture. It may be seen from Fig. 5 that for this system, the derived values of $n_s\chi$ are substantially greater than 2 in the temperature range under consideration, so one infers that miscibility is restricted to a relatively narrow range of epoxy-rich compositions, consistent with observation [1, 3]. Indeed all the linear alkanes investigated here were predicted to be of limited interest as solvents if one is seeking to obtain a material with a relatively high pore content by CIPS.

The above trends are shown explicitly in Fig. 7, where we have replotted the results in $\alpha, n_s\chi$ space for different values of ϕ_B for decane epoxy and 2,6-dimethyl-4-heptanone epoxy mixtures, which are the least miscible and most miscible systems, respectively. In the latter case, CIPS was predicted to be possible over the whole range of ϕ_B and the whole range of temperatures between 21 and 150 °C. Indeed freshly

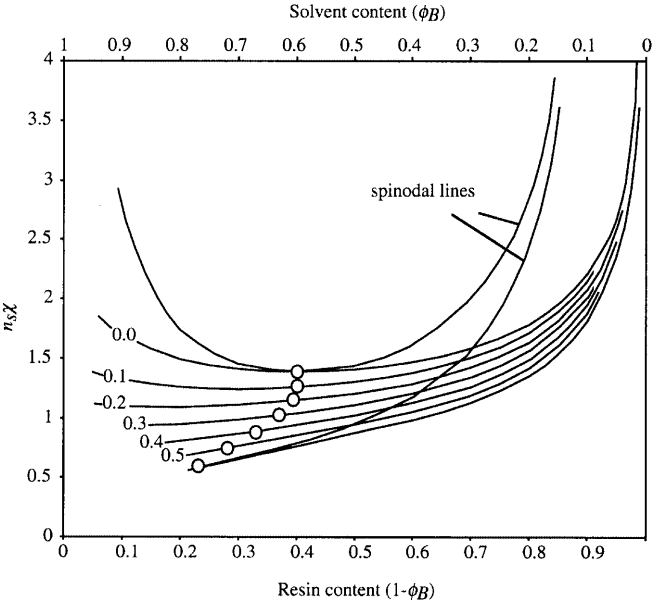

Fig. 6 Predicted cloud-point curves for a decane epoxy mixture for the degrees of conversion indicated, along with the cloud-point curve at the gel point, the spinodal curves corresponding to the gel point and to the uncured epoxy, and the critical points (*open circles*)

Table 1 Estimates of the room temperature (21 °C) interaction parameters relative to that of hexane, based on the solubility parameter approach and on the T_c measurements, as described in the text

Solvent	χ/χ_{hexane} (solubility parameters)	$V_{hexane}n_s\chi/V_Bn_{s,hexane}\chi_{hexane}$ (T_c)
Hexane	1.00	1.00
Octane	0.99	0.90
Decane	0.98	0.99
Cyclohexane	0.99	0.75
Methylcyclohexane	0.97	0.65
Dibutylether	0.58	0.53
2,6-Dimethyl-4-heptanone	0.69	0.42

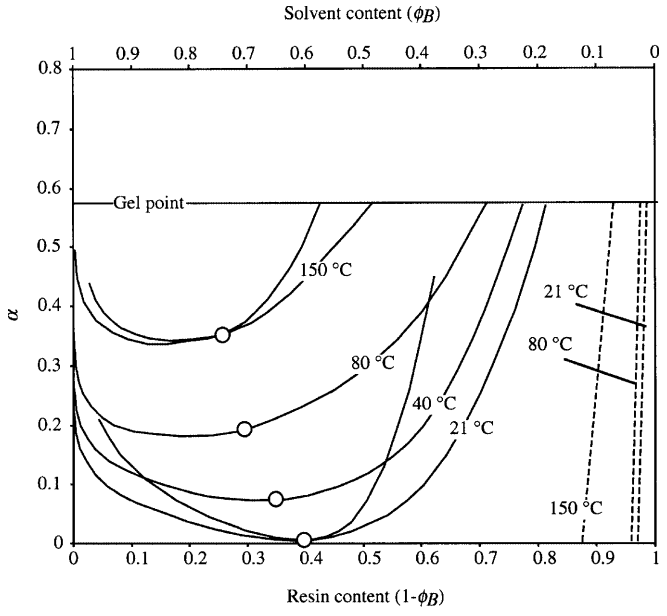

Fig. 7 Predicted cloud-point curves for decane (*hatched curves*) and for 2,6-dimethyl-4-heptanone (*solid curves*) as a function of epoxy conversion for the temperatures indicated. Critical points (*open circles*) and the spinodal curves for 21 and 150 °C are also given for 2,6-dimethyl-4-heptanone

prepared 2,6-dimethyl-4-heptanone epoxy mixtures were observed to be fully miscible at and above 21 °C. The results are also consistent with those of previous work in which the broad range of miscibility of this system was exploited to generate a wide variety of postcuring morphologies using low to intermediate solvent contents [2].

According to Fig. 7, CIPS should also be possible from very dilute solutions in 2,6-dimethyl-4-heptanone, suggesting that it might be possible to obtain stable spherical epoxy particles by choosing conditions such that precipitation occurs when α is close to α_c; however, it should be borne in mind that the assumption of uniform concentration implicit in the Flory–Huggins theory will break down at high dilutions, particularly for large α, that the curing reaction will not only be retarded at high dilutions, but also by potentially significant departures from stoichiometry in the phase-separated domains once precipitation has occurred [15] and that the concentration dependence of χ may lead to large systematic errors when the present model is used to extrapolate over wide ranges of composition. In practice it was found to be possible to obtain spherical epoxy particles at low dilutions and high temperatures, but they remained "sticky" even after relatively long curing times. In the absence of stirring they rapidly agglomerated and cocontinuous structures such as that shown in Fig. 8 settled out of the solution.

After evaporation of the excess solvent and postcuring at 80 °C, followed by drying under vacuum, it was possible to obtain rigid foams from the particle agglomerates precipitated from dilute solution. On the other hand, if one wishes to exercise direct control over the pore volume fraction by varying the initial solvent volume fraction, it is arguably better to work at $\phi_B < \phi_c$, where the epoxy-rich phase should be continuous at least in the early stages of phase separation. At and around a solvent volume fraction of 50% the morphology will nevertheless tend to evolve towards a cocontinuous structure, regardless of the initial phase-separation mechanism, so some degree of kinetic control is necessary in order to produce closed cell foams under these conditions. Based on Fig. 7, one possible approach might be to heat-treat a blend containing 50% solvent at 150 °C until α is close to α_c (i.e., where there is a significant increase in viscosity) and then to cool the sample so that it passes through the metastable regime of the phase diagram at some intermediate temperature, such that nucleation and growth of solvent-rich domains is able to take place, but their coalescence is limited. The result of air-cooling from 150 °C to room temperature after partial curing at 150 °C is shown in Fig. 9. After standing for a few days at room temperature, the sample was postcured at 80 °C and dried under vacuum to give a closed-cell foam with a pore volume fraction approaching 50 % (isothermal curing under these conditions results in a cocontinuous morphology [2]).

Another phase diagram of practical interest for CIPS in epoxy resins is that of cyclohexane (Fig. 10). Although the range of miscibility is in this case predicted to be somewhat reduced compared with that of 2,6-dimethyl-4-heptanone, it is substantially greater than that of the linear alkanes, including hexane, as again reflected by the variety of morphologies which can be obtained from this system [1]. This indicates that altering the configuration of a relatively inert nonpolar structure provides an effective alternative to increasing the polarity at fixed molar volume when looking to improve the range of compositions for which CIPS is feasible within a given temperature range.

Conclusions

The thermal gradient oven provides a rapid and simple means of determining points in composition–temperature space corresponding to the transition from homogeneous to heterogeneous postcuring microstructures. In using this data to estimate $\chi(T)$ our main assumption was that this transition coincides with the cloud-point curve corresponding to the gel point of the resin. Moreover, for the present purposes we also assumed that $\chi(T)$ is independent of composition and that the molar mass distribution of the epoxy resin may be approximated using a simple statistical branching model, both of which would need to be reconsidered in a

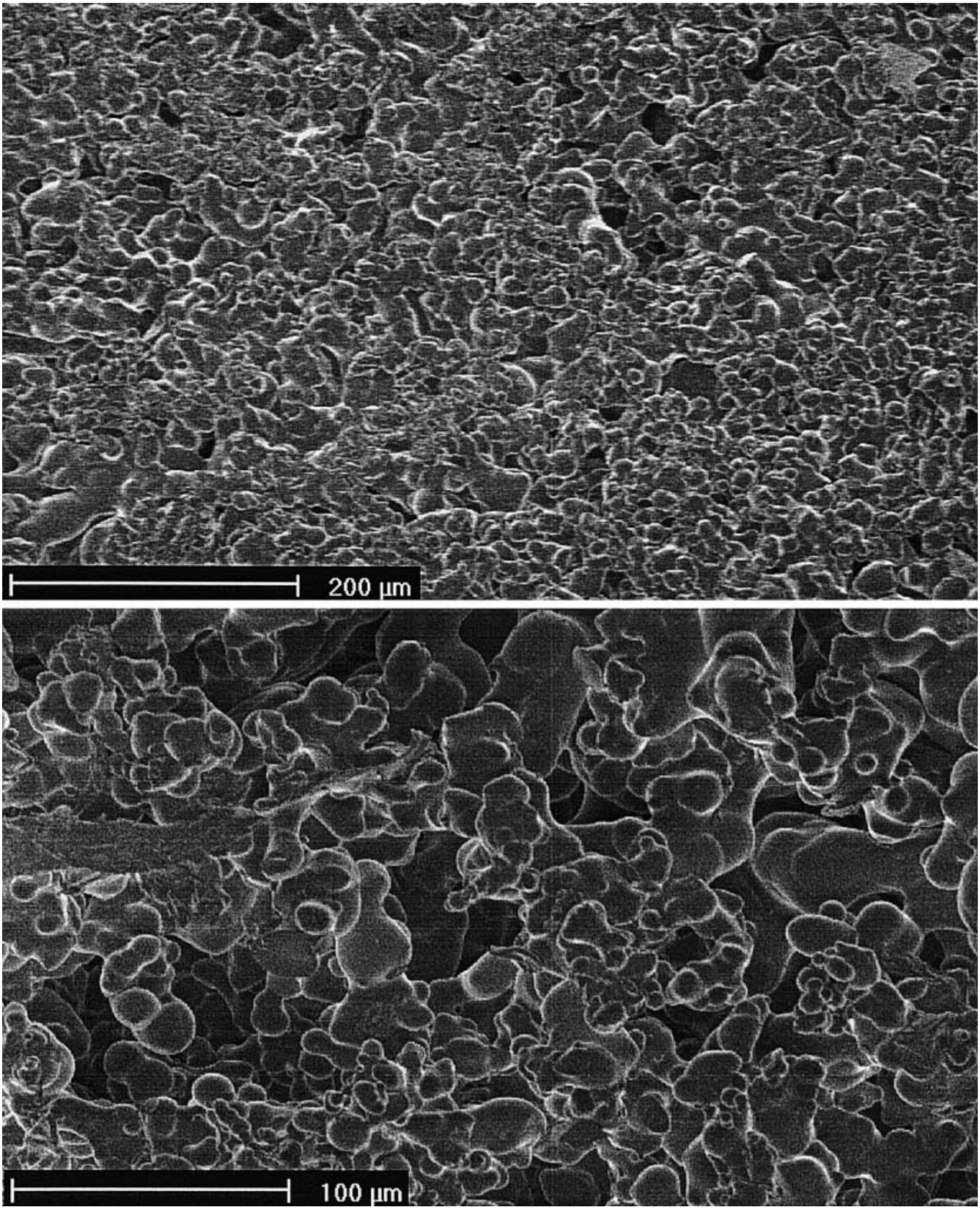

Fig. 8 Microstructure of the precipitate from a 5% epoxy 2,6-dimethyl-4-heptanone solution cured at 150 °C and postcured at 80 °C

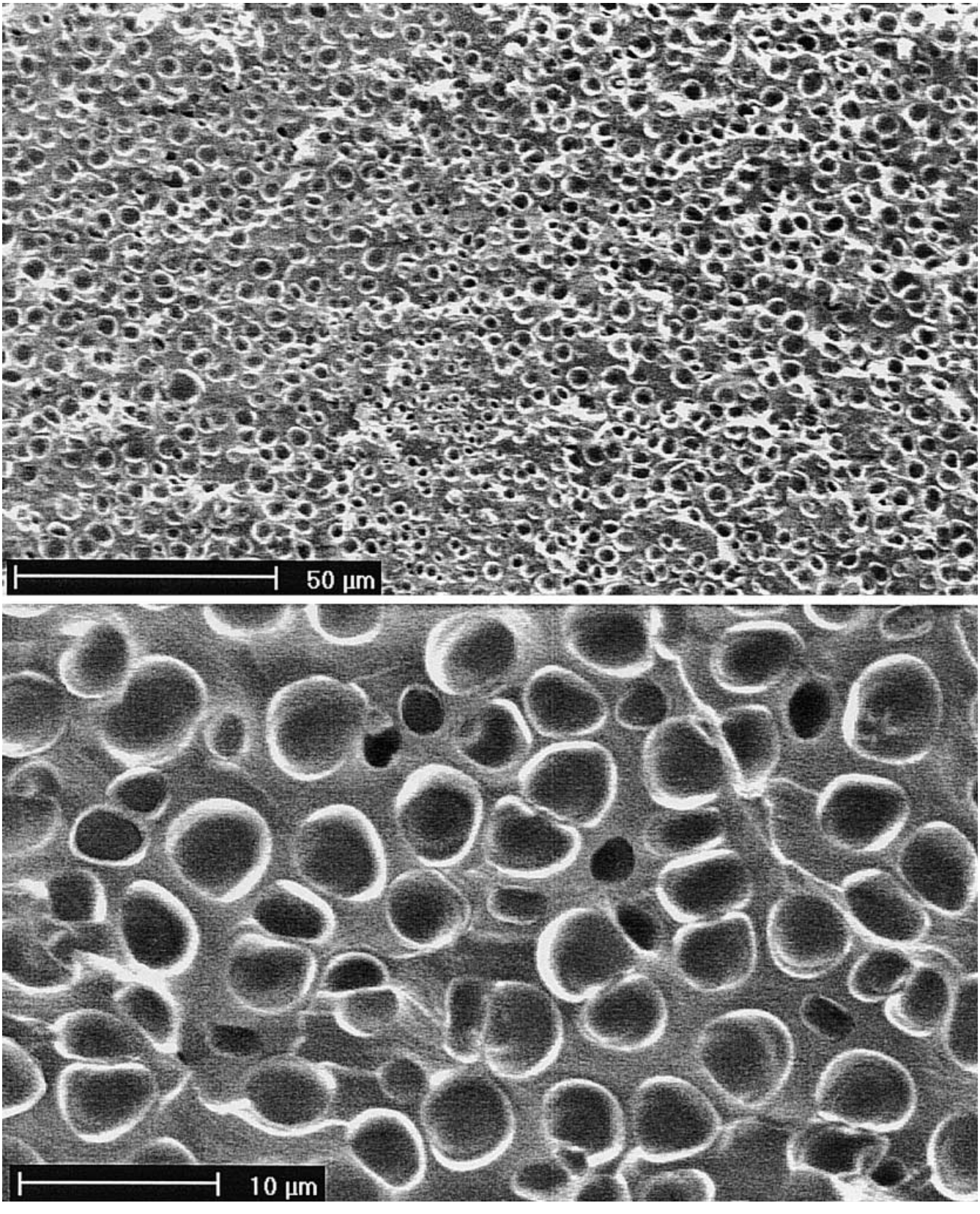

Fig. 9 Microstructure of a 50% epoxy 2,6-dimethyl-4-heptanone mixture partially cured at 150 °C, cooled to 21 °C and postcured at 80 °C

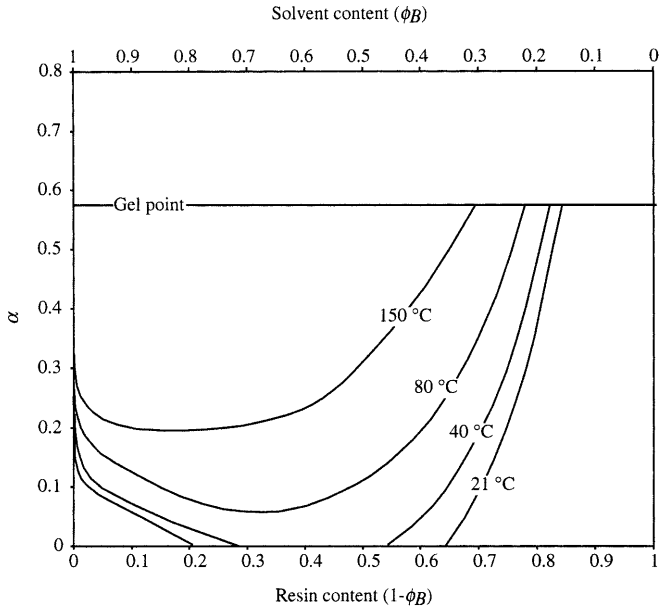

Fig. 10 Predicted cloud-point curves for cyclohexane as a function of epoxy conversion for the temperatures indicated

more detailed approach (detailed discussion of these points is beyond the scope of the present work). However, we believe the results to be of practical interest in that even a very approximate idea of the relevant phase diagrams permits a rational approach to the control of the morphologies of macroporous thermosets prepared by CIPS, as briefly illustrated here, requiring only inexpensive equipment.

Acknowledgements The authors would like to thank J.G. Hilborn, W. Dufour and R. Porouchani for their contributions to this work.

Appendix

The relevant formulae are given here for the case where Eq. (8) is assumed to describe the free energy of mixing (the case of Eq. (6) is described elsewhere). In a multicomponent blend, the spinodal curve is given by

$$n_s\chi = \frac{1}{2\phi_B} + \frac{1}{2(1-\phi_B)n_e\bar{N}_w} \quad , \tag{A1}$$

where

$$\bar{N}_w = \frac{\sum_N NP(N)}{\sum_N P(N)} \quad . \tag{A2}$$

At the cloud point, it may be shown that

$$\frac{\sigma}{2}(1+v_o) + \left(1 - \frac{1}{n_e\bar{N}_n}\right) - v_o\left(1 - \frac{1}{n_e\bar{N}''_n}\right) + \left(\frac{1}{1-\phi_B} - \frac{1+v_o}{2}\right)\ln\left(\frac{\phi_B}{\phi''_B}\right) = 0 \quad , \tag{A3}$$

with

$$\sigma = 2n_s\chi(\phi''_B - \phi_B) + \ln\left(\frac{\phi_B}{\phi''_B}\right) \quad , \tag{A4}$$

$$v_o = \frac{1-\phi''_B}{1-\phi_B} \quad , \tag{A5}$$

$$\bar{N}_n = \frac{\sum_N P(N)}{\sum_N \frac{P(N)}{N}} \quad , \tag{A6}$$

$$1 - \phi''_B = (1-\phi_B)\sum_N P(N)\exp(-\sigma n_e N) \tag{A7}$$

and

$$\bar{N}''_n = \frac{\sum_N P(N)\exp(-\sigma n_e N)}{\sum_N \frac{P(N)\exp(-\sigma n_e N)}{N}} \tag{A8}$$

(the double primes refer to the incipient phase). For a given α and hence for a given $P(N)$ Eq. (A1) may be solved numerically for any given ϕ_B by varying the separation factor, σ, subject to the condition that for $\phi_B > \phi_B^{crit}$, $\sigma < 0$ and for $\phi_B < \phi_B^{crit}$, $\sigma > 0$, where the composition at the critical point, ϕ_B^{crit}, is given by

$$\phi_B^{crit} = \left(1 + \frac{(n_e\bar{N}_z)^{1/2}}{n_e\bar{N}_w}\right)^{-1} \quad , \tag{A9}$$

with

$$\bar{N}_z = \frac{\sum_N P(N)N^2}{\sum_N P(N)N} \quad . \tag{A10}$$

$n_s\chi$ may then be determined from Eq. (A2).

References

1. Kiefer J, Hilborn JG, Hedrick JL (1996) Polymer 37:5715
2. Kiefer J, Hedrick JL, Hilborn JG (1999) Adv Polym Sci 147:161
3. Kiefer J, Hilborn JG, Månson J-AE, Leterrien Y, Hedrick JL (1996) Macromolecules 29:4158
4. Kiefer J (1997) Lausanne Federal Institute of Technology
5. Konigsveld R, Kleintjens LA (1971) Macromolecules 4:637
6. Lipatov YS, Nerzerov AE (1997) Thermodynamics of polymer blends. Technomics, Lancaster, USA
7. Brandrup J, Immergut EH (1989) Polymer handbook. Wiley, New York
8. Dusek K, MacKnight WJ (1988) In: Dickie RA, Labona SS, Bauer RS (eds) Crosslinked polymers. ACS Symposium Series 367. American Chemical Society, Washington, DC

9. Williams RJJ, Rozenberg BA, Pascault J-P (1977) Adv Polym Sci 128:95
10. Flory PJ (1942) J Chem Phys 10:51
11. Huggins ML (1942) Ann NY Acad Sci 42:1
12. Koningsveld R, Staverman AJ, (1968) J Polym Sci Part A2 6:325
13. Stockmayer WH (1944) J Chem Phys 12:45
14 Flory PJ (1953) Principles of polymer chemistry. Cornell University Press, Ithaca
15. Clarke N, McLeish TCB, Jenkins SD (1995) Macromolecules 28:4650
16. Van Krevelen DW (1976) Properties of polymers. Elsevier, Amsterdam